Investigation of distribution uniformity of distributor for biogas slurry application based on CFD analysis

Jingjing Fu, Yongsheng Chen, Binxing Xu, Biao Ma, Pengjun Wang, Aibing Wu, Mingjiang Chen*

(*Nanjing Institute of Agricultural Mechanization, Ministry of Agriculture and Rural Affairs, Nanjing 210014, China*)

Abstract: A horizontal distributor for biogas slurry application was proposed to explore the distribution performance through CFD analysis and verified by field test. The rheological properties of biogas slurry were analyzed at first, and key parameters were obtained for the next simulation. The effects of distribution modes, inlet direction, and outlets number on the velocity distribution of flow field and mass flow rate of the horizontal distributor were investigated by CFD simulations. Results of rheological properties indicated that biogas slurry was a non-Newtonian fluid and exhibited shear-thinning behavior. It can be well described by power-law model. The simulation results showed that the geometry of rotor, especially the block numbers was the main factor that determined the fluid movement and trajectory of distribution and output. The mode rotor 1 with two blocks reached the lowest variable coefficient of mass flow rate (4.49%), indicating a higher degree of uniformity. The upward inlet direction would obtain less dead zone, and the distributor with an even outlets number would possess more uniform distribution and less dead zone. The field test of the distributor with rotor 1, upward inlet direction, and 24 outlets has been carried on to verify the simulation results, the variable coefficient of mass flow was 13.06%, which was slightly higher than the simulation (9.23%), but it still within the range of requirement (<15%). The proposed model and the findings of this work are of guiding significance for the study of the utilization technology and equipment of liquid biogas residue.

Keywords: distributor, biogas slurry, distribution uniformity, rheological properties, CFD

DOI: 10.25165/j.ijabe.20231601.7460

Citation: Fu J J, Chen Y S, Xu B X, Ma B, Wang P J, Wu A B, et al. Investigation of distribution uniformity of distributor for biogas slurry application based on CFD analysis. Int J Agric & Biol Eng, 2023; 16(1): 45–52.

1 Introduction

Intensive livestock production yields vast quantities of manure, especially in China, the total amount of livestock and poultry manure reaches 40×10^8 t/a, while the effective processing capacity is less than 50%[1-3]. The development of the biogas industry through anaerobic digestion has already solved some of the problems in the treatment of livestock and poultry manure, and simultaneously alleviated the demand for energy[4,5]. However, the improper treatment of biogas residue may affect the normal operation of biogas projects, and cause secondary pollution either[6,7]. The biogas residue, used as a basal fertilizer returning to the field has become an important and main treatment means[8]. In general, the technology and equipment of liquid biogas fertilizer are immature, thus limiting the comprehensive utilization of biogas residue.

The application of organic fertilizers has gradually been paid attention to in recent years. Most organic liquid fertilizers are spread in a rougher way, mainly including direct spray and flood irrigation. While those patterns will pollute the environment and the fertilizer utilization rate is low. The multiplexing application techniques and equipment of liquid fertilizer are developed nowadays. That equipment is mainly composed of tank, distributor, and application device[9-11]. Usually, the solid components in the liquid slurry are more complex and had a higher viscosity. After filling the tank, the liquid slurry is pumped into the distributor and further evenly delivered to the application device with multiple pipelines, finally returning to the field. The spreading methods depend on the different application devices. The distributor plays a key role in the liquid slurry spreader. The uniform distribution technology of liquid slurry with high impurity content is a prerequisite for continuous flow, stable delivery, and spreading performance in the whole operation process. Recently, some studies have just been carried out on the technology and equipment of liquid fertilizer spreaders. Most of those studies are aimed at deep application-type devices[12-14]. The distributor, as the most important device in the whole equipment, has its main function is to realize the even distribution and continuous flow of liquid fertilizer in multiple pipelines. Currently, the research on the distributor mainly focuses on the structural design to solve cooperation and blockage issues between distributor and application device[15,16]. Except for the reasonable structural design, the coupling relationship between distribution structure and physical characteristics of liquid slurry has a significant influence on the performance of distributor. The rheological behavior of liquid manure has been studied by many researchers. Liquid manure is a non-Newtonian material and it behaves like a

Received date: 2022-02-28 **Accepted date:** 2023-01-02

Biographies: Jingjing Fu, PhD, Assistant Researcher, research interest: technology and equipment for utilization of agricultural waste, Email: tutujing12@163.com; **Yongsheng Chen**, BS, Researcher, research interest: technology and equipment for utilization of agricultural waste, Email: cys003@sina.com; **Binxing Xu**, MS, Assistant Researcher, research interest: technology and equipment for utilization of agricultural waste, Email: 702076554@qq.com; **Biao Ma**, MS, Assistant Researcher, research interest: technology and equipment for utilization of agricultural waste, Email: 949704383@qq.com; **Pengjun Wang**, MS, Assistant Researcher, research interest: technology and equipment for utilization of agricultural waste, Email: wjok-000@163.com; **Aibing Wu**, BS, Associate Researcher, research interest: technology and equipment for utilization of agricultural waste, Email: 454666341@qq.com.

***Correspondence: Mingjiang Chen**, MS, Associate Researcher, research interest: technology and equipment of utilization of agricultural waste. Nanjing Institute of Agricultural Mechanization, Nanjing 210014, China. Tel: +86 25-84346003, Email: cmj_cn@163.com.

pseudoplastic liquid[17-19]. Investigation of rheological property of liquid slurry and the selection of rheological model are an important basis for the design and optimization of the operation efficiency of distributor. While there are few literatures on both geometry of distributor and rheological properties of liquid slurry.

To address the abovementioned issues, a horizontal distributor was proposed with different distribution modes, inlet direction, and outlets number in this study to achieve a uniform distribution for biogas slurry application. The effects of total solid (TS) content and rotational speed on the rheological property of biogas slurry were evaluated, and the fluid type and rheological model of biogas slurry were determined for further simulation. The kinetic and distribution characteristics of biogas slurry were analyzed by establishing a fluid-solid coupling model of distributor and biogas slurry using computational fluid dynamics (CFD) method. The effects of distribution modes, inlet direction, and outlets number on the distribution uniformity of each outlet pipeline of distributor were investigated. Finally, the simulation results were compared with the results of field test. Hence, we expect the findings of this work could improve the utilization of technology and equipment for biogas residue and promote sustainable development.

2 Materials and methods

2.1 Materials

Biogas slurry (without solid-liquid separation) was collected from a small-scale biogas project in Jining, Shandong Province, China. The biogas slurry was fermented in a fermenting tank after the biogas project was complete so that the biogas slurry used in this work could be directly used as organic fertilizer. The original TS content and density of biogas residue were 10.61% and 1.24 g/cm^3, respectively. In order to investigate the effects of TS on the rheology and flow characteristics in the distributor, samples were diluted with water to the TS content of 2%, 4%, 6%, 8%, and 10%.

2.2 Design of distributor

This study designed a distributor with horizontal structure as shown in Figure 1a. The in-out direction of this distributor follows the "one in (vertical direction)-two sides out (horizontal direction)" mode. In order to explore the kinetic and distribution characteristics of biogas slurry inside the distributor and its distribution uniformity, different inlet direction (upward, middle and downward), distribution rotors (rotor 1, rotor 2, and rotor 3, Figure 1b), and outlet numbers (12, 18 and 24) were proposed.

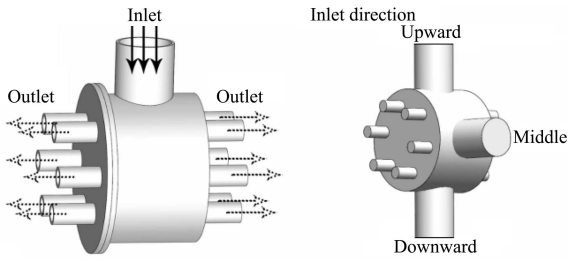

a. Distributor with horizontal structure

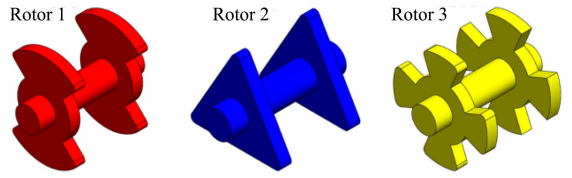

b. Rotors with different distribution modes

Figure 1 Structure of distributor with three different distribution modes

Their working principle is that through the rotation of rotor, the blocks sweep the outlets intermittently to generate pulsed high pressure, and evenly transport the biogas slurry to each outlet.

2.3 Characterization of biogas slurry

The TS contents of biogas slurry were measured according to the standard methods from the American Public Health Association[20].

The densities of samples were tested using a gravitometer (Hengshui Chuangji Instrument Co., Ltd., China). The results were represented by three replications.

The rheological measurements of biogas slurry with different TS contents were performed using an NDJ-8S digital rheometer (Shanghai Jitai Electronic Science and Technology Co., Ltd, China) under room temperature. After evenly stirring, all samples were tested at five different rotational speeds (3, 6, 12, 30, and 60 r/min) over a period of 100 s for capturing the flow behavior.

For the efficient simulation of the rheological characteristics of biogas residue, the most commonly used models, the Bingham, Ostwald (power-law model), and Herschel-Buckley (H-B) were selected and analyzed in this work according to the following equations[21]:

$$\tau=\tau_0+\mu_B\cdot\gamma \quad (1)$$

$$\tau=K\cdot\gamma^n \quad (2)$$

$$\tau=\tau_0+K\cdot\gamma^n \quad (3)$$

where, τ is the shear stress, Pa; τ_0 is the yield stress, Pa; μ_B is the Bingham viscosity coefficient, Pa·s; γ is the shear rate, s^{-1}; K is the consistency index, Pa·s^n; n is the flow behavior index.

The fluid motion of biogas slurry is very complex, with irregular behavior both in time and in space, so statistical descriptions are often needed. Usually, the Reynolds number (Re) is used as a criterion for judging the flow state of a viscous fluid. But there is no theorem directly relating Re to turbulence. Typically, flows are turbulent if the Re is greater than 2320, and are laminar if it is less than 2320[22]. Re of the fluid in the distributor can be accordingly expressed as:

$$Re=\rho\cdot u\cdot d/\mu \quad (4)$$

where, ρ is fluid density, kg/m^3; u is mean flow velocity, m/s; d is distributor diameter, m; μ is fluid dynamic viscosity, Pa·s.

2.4 CFD simulation

According to the design of the distributor, numerical models of operational process of distributor and flow characteristics of biogas slurry were established for simulations via CFD using the ANSYS 2020 R2 (Table 1). To develop the CFD simulation, three main steps are performed: the design of the distributor geometry, mesh generation, and the selection of the physical models and solvers.

Table 1 Parameters design table for the simulation

Parameters	Level		
Distribution modes	Rotor 1	Rotor 2	Rotor 3
Inlet direction	Upward	Middle	Downward
Outlets number	12	18	24

2.4.1 Geometry and meshing

The 3D model of distributor was set up in the software SOLIDWORKS 2020. After importing the 3D model, the geometry and meshing of the shell and rotor were generated using DesignModeler and Meshing modules in ANSYS Workbench 2020 R2. Mesh sensitivity is traditionally investigated by varying a model's mesh discretization level to determine whether its response is qualitatively affected. The number and quality of mesh used for discretizing the model play crucial roles in accuracy. Mesh quality was assessed by the skewness values, which could be calculated by the statistic function built in the Meshing module.

Generally, the skewness value <0.95 is recommended. In this study, the selection of mesh element size was based on body and face sizing methods using tetrahedral meshes, all three modes possessed very low skewness values (rotor 1 was 0.268, rotor 2 was 0.259, rotor 3 was 0.267), which represented "excellent" mesh quality level.2.4.2 Computational domain and solution

In this study, the finite volume method (FVM) is used for discretization equations. The simulation model used to describe the biogas slurry in the distributor is developed with the following assumptions: 1) single-phase model; 2) 3-D incompressible and isothermal non-Newtonian fluid; 3) no reverse flow. Dynamic viscosity and density are required to conduct numerical simulations. The model (laminar or turbulence model) selection was based on the *Re* of the fluid. The sliding mesh (SM) approach was used to calculate the effects of a rotational flow at the rotor and inner surface of the shell. The rotational speed of the rotor was set to 120 r/min. The boundary conditions were defined by setting the inlet flow velocity to 3 m/s and flow at the outlet as fully-developed. All the distributor walls were marked with a non-slip condition. The solution method for pressure-velocity coupling equations (Coupled) algorithm was used for the calculation. Each numerical simulation is carried out for transient conditions with total time steps of 1000 with a time step of 0.01 s.

3 Results and discussion

3.1 Rheological characteristic of biogas slurry

3.1.1 Effect of solid content on rheological characteristics

The viscosity curves of biogas slurry with different solid contents under various rotation speeds were shown in Figure 3. And the density of biogas slurry is listed in Table 1. It can be seen from Figures 2a-2e that all samples possessed relatively stable viscosity data at each rotational speed in the limited test time, which represented lower experimental noise. On the other hand, each set of biogas slurry presented decreased tendency with increasing rotational speed, which is so-called the "shear-thinning" behavior. Combined with the data of average viscosity (Figure 3f), the higher the solid content, the larger oscillation of the increased magnitude of viscosity. And biogas slurry with higher solid content processed larger viscosity. The biogas slurry usually contains entangled fibers and some fine or coarse particles, especially with high TS content (The higher TS content manifest larger density, Table 2). That is due to the colloids originating from manure, particles with various grain sizes as well as long fibers like blades and culms from straw. Those above phenomena that happened in rheological experiments might be ascribed to the particle-particle and particle-dispersion medium interactions: at higher rotational speed, phase separation was easier to occur and large solid particles clung to the ribbon in the sample with higher solid content. That indicated that the biogas slurry underwent a solid phase rotation. The results obtained in this paper agree qualitatively with literature data[23-25]: the rheological properties of biogas slurry are found to exhibit pronounced dependency on solid content, but there is no functional correlation between viscosity and TS content. The viscosity of biogas slurry varied greatly on the "thick" or "thin" network formed by the large molecules, such as undigested lignocellulosic materials suspended in the slurry. Alternatively, this might also indicate that the TS content of a non-Newtonian sludge is not a suitable indication of viscosity due to the disproportionately large role solute and colloid interactions have on the rheological characteristics.

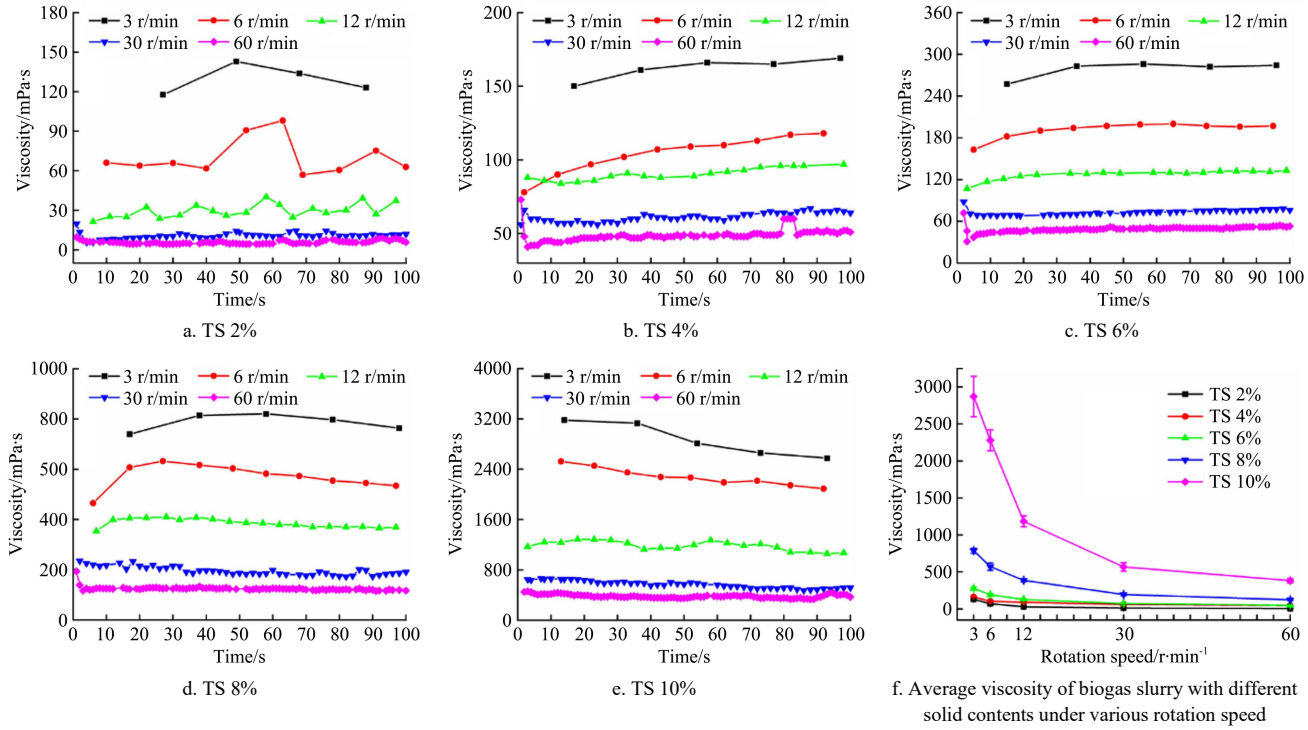

Figure 2 Viscosity of biogas slurry with different solid contents under various rotation speeds

Table 2 Density of biogas slurry with different solid content

TS content/%	2	4	6	8	10
Density/kg·m^{-3}	999.25 (2.75)	1012.67 (6.42)	1029.33 (1.15)	1044.67 (3.79)	1129.33 (33.29)

Note: The data in parentheses are the standard deviation.

3.1.2 Model identification for describing the rheological properties

In suspended liquids, such as biogas slurry, the non-Newtonian behaviors are believed to be originated mainly from the colloidal properties. Some researchers have divided the characterization of the rheological behavior of suspended liquids into three steps: 1)

viscometry, 2) rheological modeling, and 3) correlation of the parameters[26]. To further quantify the non-Newtonian behaviors, the Bingham, Ostwald (power-law model), and Herschel-Buckley (H-B) (Equations (1)-(3)) were fitted according to the experimental data to seek a better one for describing the flow. And before the model simulation, the shear stress and shear rate are needed.

In this study, the rotational rheometer with the geometry of concentric cylinders was used for testing the viscosity. In the testing process, the fluid is placed in a gap between an inner cylinder (rotor) and an outer cylinder (cup). The inner cylinder is rotated, while the outer one is stationary, the system is referred to as Searle-system. Given the rotational speed N (s^{-1}), the torque M (N·m) and viscosity (Pa·s) are obtained. The shear stress and shear rate related to the surface of the inner cylinder are calculated with the following equations:

$$\tau_i=M/(2\pi\cdot L\cdot R_i^2) \quad (5)$$

$$\gamma_i=4\pi\cdot N\cdot R_e^2/(R_e^2-R_i^2) \quad (6)$$

where, L is the height of the rotor, m; R_i and R_e are the radii of the inner and outer cylinder (m), respectively. Hence, the viscosity is given by

$$\eta=M\cdot(R_e^2-R_i^2)/(N\cdot 8\pi^2\cdot L\cdot R_e^2\cdot R_i^2) \quad (7)$$

The shear stress and shear rate were then calculated with the results illustrated in Table 3. It can be found that except for the sample TS 2%, all other four samples showed similar trends: a higher shear rate led to higher shear stress, and the higher the TS, the higher the shear stress. The shear stress increased by 9.36-24.75 folds when the TS increased from 4% to 10%. As above analysis, the intrinsic mechanism is about the particle interactions. An increment of TS can decrease the distance between the particles of biogas slurry, increase their interactions, and subsequently enhance the resistance of slurry to flow when subjected to shear[27]. While for the very low solid content condition, it might be the hydrodynamic interactions was the substantial factor that influenced the rheological properties[28].

Table 3 Shear rate and shear stress of biogas slurry with different solid contents

Rotational speed /r·min^{-1}	TS content/%									
	2%		4%		6%		8%		10%	
	Shear rate /s^{-1}	Shear stress /Pa	Shear rate /s^{-1}	Shear stress /Pa	Shear rate /s^{-1}	Shear stress /Pa	Shear rate /s^{-1}	Shear stress /Pa	Shear rate /s^{-1}	Shear stress /Pa
3	3.21	0.42	0.76	0.12	0.76	0.21	0.76	0.60	0.87	2.49
6	6.42	0.45	1.52	0.16	1.52	0.29	1.52	0.87	1.74	3.96
12	12.85	0.38	3.04	0.28	3.04	0.39	3.04	1.17	3.47	4.11
30	32.12	0.35	7.61	0.47	7.61	0.55	8.68	1.70	8.68	4.93
60	64.25	0.375	15.22	0.74	15.22	0.74	17.36	2.16	17.36	6.63

Based on the calculated data of shear rate and shear stress, the parameters of each model together with the R^2 value in the correlation are displayed in Table 4. Higher R^2 value demonstrated a better accuracy for describing the flow of biogas slurry. As shown in Table 4, the negative τ_0 value obtained from the H-B equation simulation under 6% and 8% solid content conditions, indicating that the H-B model was inefficient in simulating the effect of TS content on the rheological properties of biogas slurry. Conversely, the power-law model fit was superior to that of the other two models. The Bingham model has a linear relationship between shear stress and shear rate, the shear-thickening behavior of the suspension is not considered. This also can be proved by the higher R^2 value of the power-law model in comparison with the Bingham model (0.44924-0.99951 versus 0.21468-0.98427). Additionally, except for the sample with TS 2%, all the other samples revealed better fitting degree (R^2 value close to 1) of the power-law model in simulating the rheological properties. As verification of the experimental and calculated shear rate and shear stress data, the significant variation in the viscosity could not be observed in the sample with very low solid content. That might reflect the different flow behavior compared with samples of higher solid contents. The consistency index (K) reflected the intensity of the material in the non-linear regime[29]. And n is a dimensionless parameter to represent the flow behavior index. When n is close to 1, the fluid property gradually tends towards the behavior of Newtonian fluid. Also except for the TS 2%, the TS content increased could increase K and decrease n. It suggests that as the solid content increases, the fluid type of sludge gradually changes from a Newtonian fluid to a non-Newtonian fluid and demonstrated a strengthened non-Newtonian flow characteristic.

In conclusion, the power-law model was selected as the rheological model of biogas slurry for further CFD simulation.

Table 4 Model parameters under various TS contents

Equation	Parameter	TS content/%				
		2	4	6	8	10
Bingham	τ_0/Pa	0.41744	0.11402	0.24139	0.75040	3.07516
	μ_B/Pa·s	–0.00104	0.04249	0.03487	0.08747	0.20977
	R^2	0.21468	0.98427	0.94206	0.90007	0.86071
Power law	K/Pa·s^n	0.46709	0.13121	0.24264	0.73517	2.92794
	n	0.06657	0.63490	0.41071	0.38131	0.27616
	R^2	0.44924	0.99715	0.99951	0.99371	0.91361
Herschel-Buckley	τ_0/Pa	18.93461	0.02761	–0.02143	–0.97167	0.12911
	K/Pa·s^n	–18.47325	0.10897	0.26275	1.67379	2.80337
	n	0.00140	0.69079	0.39133	0.21858	0.28454
	R^2	0.17005	0.99658	0.99938	0.99935	0.87043

3.2 CFD analysis

3.2.1 Determination of CFD simulation settings

The rheological properties of biogas slurry with TS=8% was determined in all simulation. According to Equation (4), the biogas slurry TS=8% was considered as turbulent flow for the Re>2320, Realizable k-ε was applied as the turbulent model. And the values of density, K, and n (Power law model) are needed to complete the Materials setting.

3.2.2 Flow performance of different distribution modes

The fluid motion in the axial direction was the dominant fact that affected the distribution of the biogas slurry. Hence, the axial velocity on the mid-vertical surface (centrosymmetric plane) was selected to do the comparison. The velocity vectors and contours of different distribution modes on the centrosymmetric plane and the velocity contours of inner wall of shell are displayed in Figure 3. The condition of all three modes was chosen at the final step of the

simulation. It can be seen from Figure 3a that four obvious circulation cells were observed in all three modes, which indicated similar distributions of flow pattern. In Figure 3b, the velocity contour of all the modes can be divided into three magnitude zones: low (dark blue), medium (green and blue-green), and high velocities (red and yellow). The velocity close to the rotor center and outermost ring of shell were higher, which was correlated to the liquid turbulence. In the simulation of fluid models, such as stirring, mixing, or rotating conditions, the dead zone is used as an indicator that reflects the function of device geometry and fluid rheology. Dead zone refers to a region where the velocity magnitude is less than 5% of the maximum velocity[30]. In this work, the low zone could be considered as dead zone. Mode rotor 1 possessed the least dead zones at centrosymmetric plane, followed by rotor 2, and rotor 3. From the velocity contour of the inner walls of shell (Figure 3c), the velocity of both sides of each mode was similar, indicating the flow output on both sides of each distribution mode is relatively uniform. It also can be found that a larger dead zone appeared in the center axis position of all three modes, and that of rotor 1 was smaller than the other two modes. And in the outer ring of the shell, rotor 1 still had the least dead zone. It agrees with the results of the velocity contour on the centrosymmetric plane, which demonstrated that rotor 1 could fully drive the fluid to rotate in the shell and evenly transport it to each outlet. While rotor 2 had the largest dead zone at the output of the shell. It might be the rotor blocks had a small contact surface with fluid on the outer ring of the shell. Overall, from the analysis of fluid movement, it can be concluded that the distribution mode rotor 1 has shown better structural function and distribution performance.

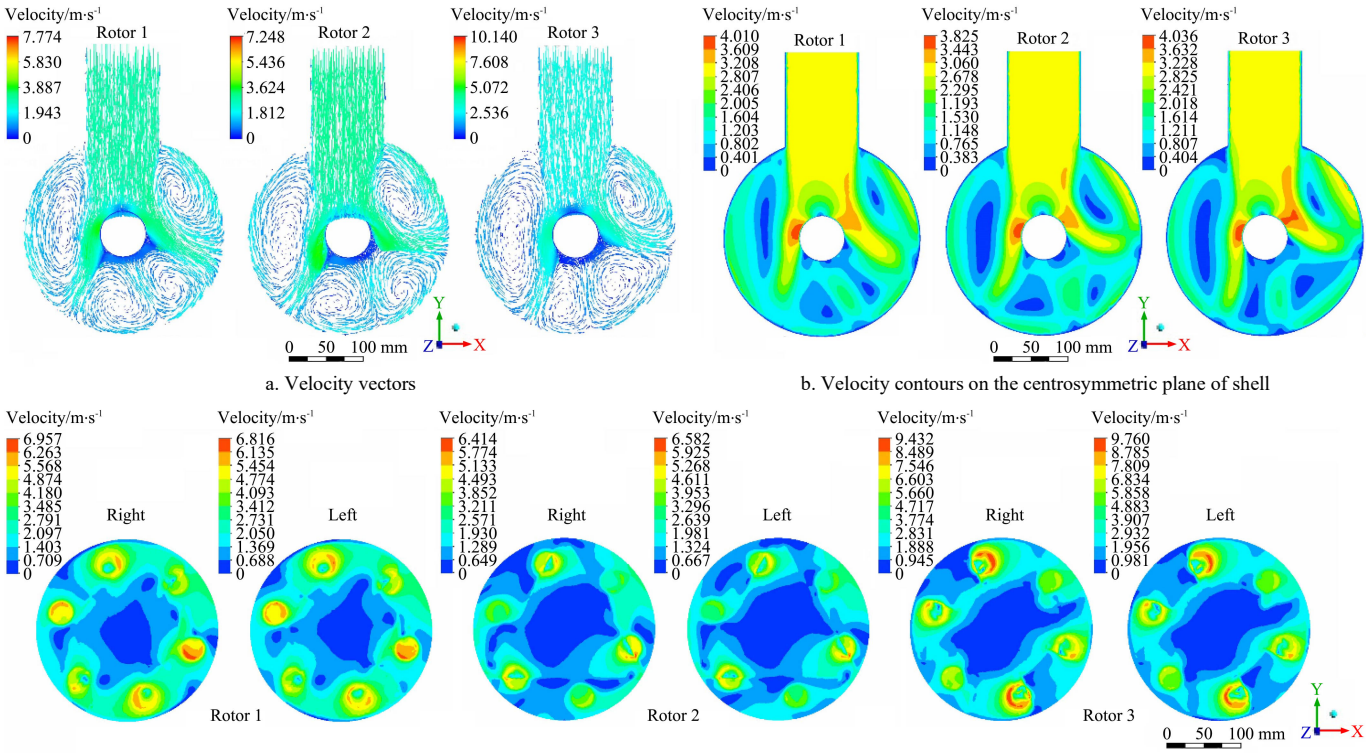

a. Velocity vectors

b. Velocity contours on the centrosymmetric plane of shell

c. Velocity contours of the inner walls of shell

Figure 3 Velocity vectors and contours of different distribution modes on the centrosymmetric plane, and the velocity contours of inner wall of shell

To quantify the distribution uniformity of different distribution modes with CFD simulation, the mass flow rate of both sides of each outlet and the total mass flow rate were monitored and calculated. In each distribution mode, the mass flow rate curves of each outlet manifested a uniform pulse fluctuation trend due to the intermittent outlet-blocking function of rotor. Hence, the same outlet of each mode and the tendency of simulation time within the initial 2 s were selected to do the comparison (Figure 4). It can be seen that obvious deviations for the three models: the frequency of mass flow per unit time of one single outlet followed the order: rotor 1<rotor 2<rotor 3. That phenomenon is ascribed to the number of blocks. Generally, in unit time, the lower the frequency, the greater the mass flow rate of each outlet at a single frequency. While the mass flow rate at each frequency followed the order: rotor 1>rotor 3>rotor 2, which is also influenced by the number of outlets that can output the liquid at each moment. The maximum number of unblocked outlets of rotor 1 and rotor 3 is 4, while that of rotor 2 is 3. And the uneven distribution velocity of fluid at the interface between the shell and outlets (Figure 3c) was also one of the reasons. From the calculation results of the average mass flow rate and variable coefficient of each outlet at each side and both sides listed in Table 5, each outlet of all three modes occurred more even mass flow data (about 2 kg/s), whether it was at each side or both sides. While the variable coefficient of flow uniformity was different among each mode: rotor 1<rotor 3<rotor 2. Hence, it can be deduced from the above results that the distribution mode of rotor 1 could achieve the best distribution uniformity.

3.2.3 Flow performance of different inlet directions

The velocity contours of distributor with different inlet directions are displayed in Figure 5. The velocity contours of two sides of the inner wall of the shell are almost the same, hence only one side is chosen to do the comparison. The velocities at centrosymmetric plane of middle and downward inlet direction (fluorescent green) are lower than that of upward direction (yellow), which is influenced by gravity. It can be seen from the velocity

contours inside the shell that their velocity distributions are similar. The main difference is at the location farthest from the inlet, the upward direction has smaller dead zone area than the other two directions. While for the velocities at the inner walls of the shell, three inlet directions shore the similar contours and dead zone areas. Only the velocity of each outlet in downward direction was slightly lower than in the other two directions. The average mass flow rates of the three inlet directions are also almost the same, and the variable coefficients are not much different (Table 6). In the above situation, the inlet direction with a smaller dead zone area is the preferred choice, and the upward inlet direction was selected.

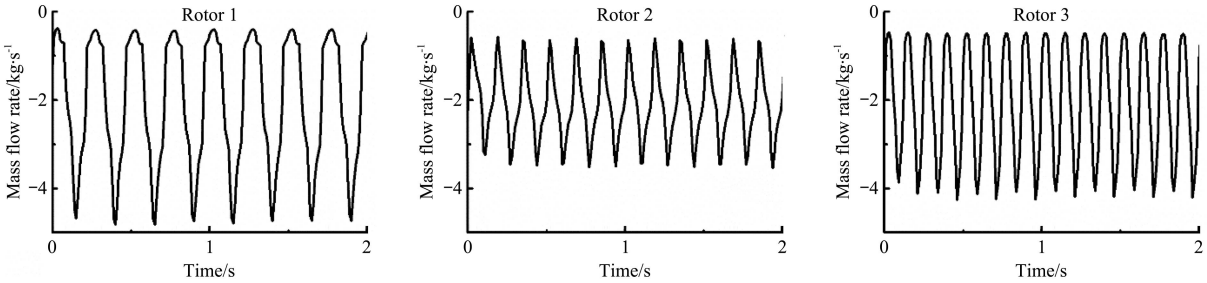

Figure 4 Mass flow rate of the same outlet of different distribution modes within initial 2 s

Table 5 Average mass flow rate and variable coefficient of each outlet

Distribution mode	Mass flow rate (right) /kg·s^{-1}	Variable coefficient (right)/%	Mass flow rate (left) /kg·s^{-1}	Variable coefficient (left) /%	Mass flow rate (total) /kg·s^{-1}	Variable coefficient (total)/%
Rotor 1	2.043(0.100)	4.89	2.05(0.092)	4.52	2.047(0.092)	4.49
Rotor 2	2.052(0.153)	7.43	2.04(0.151)	7.36	2.048(0.145)	7.06
Rotor 3	2.044(0.108)	5.29	2.05(0.106)	5.17	2.044(0.103)	5.04

Note: Variable coefficient=standard deviation/average ×100%. The data in parentheses are the standard deviation.

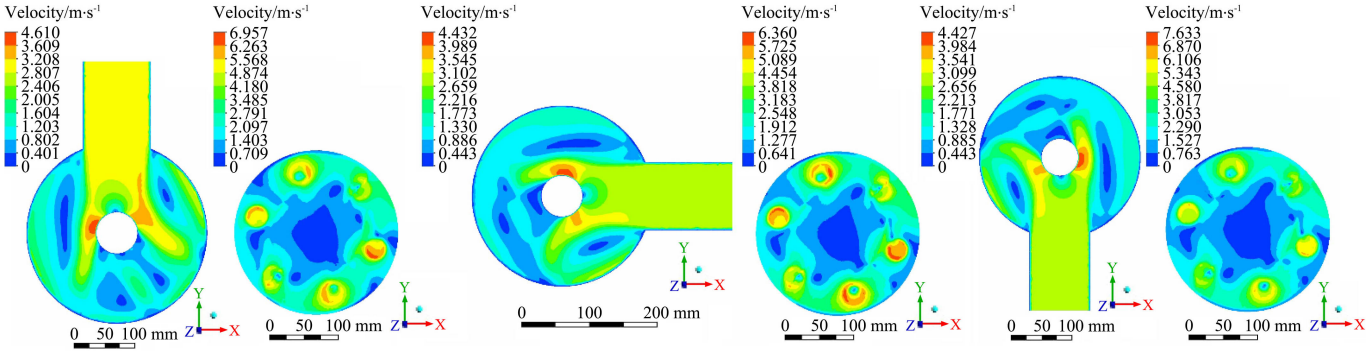

a. Upward b. Middle c. Downward

Figure 5 Velocity contours of distributor with different inlet direction located at centrosymmetric plane and the inner walls of shell (right side)

Table 6 Average mass flow rate and variable coefficient of each outlet.

Inlet direction	Mass flow rate (right) /kg·s^{-1}	Variable coefficient (right)/%	Mass flow rate (left) /kg·s^{-1}	Variable coefficient (left)/%	Mass flow rate (total) /kg·s^{-1}	Variable coefficient (total)/%
Upward	2.043(0.100)	4.89	2.05(0.092)	4.52	2.047(0.092)	4.49
Middle	2.045(0.095)	4.64	2.047(0.096)	4.69	2.046(0.092)	4.50
Downward	2.044(0.098)	4.79	2.048(0.099)	4.83	2.046(0.097)	4.74

Note: The data in parentheses are the standard deviation.

3.2.4 Flow performance of different outlets number

The velocity contours of distributors with different outlets number are exhibited in Figure 6. It is of particular noted that the distributor with 18 outlets has quite a bit of dead zone compared to the other two distributors at centrosymmetric plane. The possible reason is that although the outlets are evenly distributed relative to each outlet side, the outlets are not evenly distributed relative to the vertical direction of the inlet. This uneven distribution might decrease the smooth flow from the inlet direction, resulting in a lower flow velocity in the shell. From the velocity contours of the surface of outlet side, the three distributors all have larger dead zone areas at the central axis part, and the distribution of velocity per hole of each distributor is more even. And the outlet velocity of the distributor with 18 outlets is lower than the other two. From the data on the mass flow rate (Table 7), the average mass flow rate decreased with increasing outlets number, but the overall fluid quantity was basically the same. While the variable coefficient increased with increasing outlets number. In the practical engineering application, the uniform coefficient of variation should not exceed 15%. Therefore, on the premise of satisfying uniformity, it is possible to apply more outlets that could improve the working width and efficiency.

3.3 Field test

3.3.1 Field trial and assessment

The field test is the verification of the simulation results. From the conclusion of the CFD simulation, the distributor with an upward inlet direction and Rotor 1 (two blocks) mode were selected for the field test. And in order to increase the working width and operation efficiency, the distributor with 24 outlets was

designed (Figures 7a and 7b). The requirements of liquid fertilizer application are set to the processing capacity of up to 60 m^3/h and the uniform coefficient of variation of less than 15%. Domestic sewage was the object of this test, and the fluid volume of each outlet was recorded to assess the distribution uniformity in the field conditions.

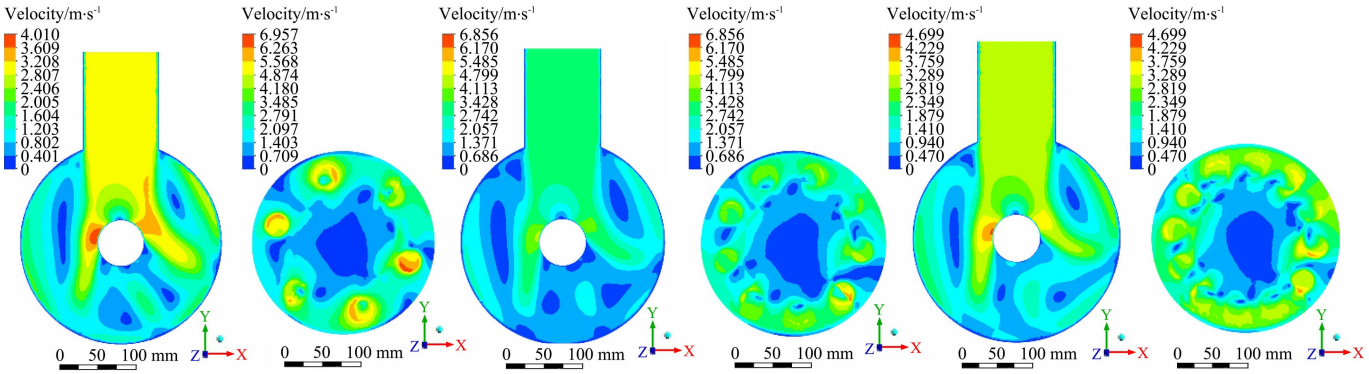

a. 12 outlets b. 18 outlets c. 24 outlets

Figure 6 Velocity contours of centrosymmetric plane and the inner walls of shell (right side)

Table 7 Average mass flow rate and variable coefficient of each outlet

Outlets number	Mass flow rate (right) /kg·s^{-1}	Variable coefficient (right)/%	Mass flow rate (left) /kg·s^{-1}	Variable coefficient (left)/%	Mass flow rate (total) /kg·s^{-1}	Variable coefficient (total)/%	Overall fluid quantity /kg·s^{-1}
12	2.043(0.100)	4.89	2.05(0.092)	4.52	2.047(0.092)	4.49	24.564
18	1.364(0.079)	5.78	1.368(0.079)	5.79	1.366(0.077)	5.61	24.588
24	1.024(0.097)	9.45	1.022(0.096)	9.44	1.024(0.094)	9.23	24.576

Note: The data in parentheses are the standard deviation.

a. Distributor b. Rotor c. Field test

Figure 7 Photos of distributor, rotor, and field test

3.3.2 Results of field test

The comparison of simulation and field test results is listed in Table 8. It can be found that whether it is the left, right side, or the overall mass flow rate, the field test results are lower than the simulation results, which is the normal efficiency loss caused by friction and resistance between components. But it should be noted that the difference in mass flow rate between the right and the left side is larger. It might be the reason that the motor had been mounted on the right side in the field test, increasing the weight on the right side. The uneven distribution of gravity would affect the uniform output of the flow, and it further increased the total variable coefficient. But overall, the field test could obtain a uniform flow distribution and the variable coefficient is within the range of requirement (<15%).

Table 8 Mass flow rate and variable coefficient of simulation and field tests

Test mode	Mass flow rate (right) /L·s^{-1}	Variable coefficient (right)/%	Mass flow rate (left) /L·s^{-1}	Variable coefficient (left)/%	Mass flow rate (total) /L·s^{-1}	Variable coefficient (total)/%
Simulation	0.98(0.093)	9.45	0.978(0.092)	9.44	0.98(0.090)	9.23
Field	0.798(0.088)	11.06	0.931(0.096)	10.34	0.865(0.113)	13.06

Note: The mass flow rate (L·s^{-1}) of simulation= mass flow rate (kg·s^{-1})/density. The data in parentheses are the standard deviation.

4 Conclusions

In this study, rheological properties of biogas slurry were analyzed and CFD method was used to simulation the distribution performance of biogas slurry inside the distribution for the biogas slurry application. And field verification test was conducted and the following conclusions are as follow:

1) The biogas slurry presented a shear-thinning behavior approved by the decreased tendency of viscosity with increasing rotational speed. The biogas slurry is believed as a non-Newtonian fluid and can be described with the power-law model. Colloid/particle interaction is the intrinsic mechanism for rheological behavior.

2) The kinetic and distribution characteristics of biogas slurry was analyzed by establishing a fluid-solid coupling model of distributor and biogas slurry using computational fluid dynamics (CFD) method. And the effects of rotor, inlet direction, and outlets number on the distribution uniformity were investigated. The rotor geometry and block numbers are the significant factors that determine the fluid distribution trajectory and output frequency.

The mode rotor 1 with two blocks possessed the least dead zones and variable coefficient of mass flow rate manifesting a better distribution function and uniformity. The inlet direction has no significant effect on the distribution uniformity, but only affects the internal dead zone area. An upward inlet direction would obtain the least dead zone. Even the number of outlets would have more uniform distribution and less dead area.

3) The field test of the designed distributor with Rotor 1, upward inlet direction, and 24 outlets could verify the CFD results. The variable coefficient of mass flow rate of 13.06% was achieved from the field test, which was within the range of requirement. It is of great significance to improve operation quality of the liquid fertilizer application.

Acknowledgements

This work was financially supported by the Jiangsu Modern Agricultural Machinery Equipment and Technology Demonstration and Promotion Project (Grant No. NJ2021-23), Jiangsu Province Agricultural Science and Technology Independent Innovation Fund Project (Grant No. CX(22)3093), the Fundamental Research Fund of the Chinese Academy of Agricultural Sciences at the Institute Level (Grant No. S202106-02), and the Key Research and Development Program of Hebei Province (Grant No. 20327313D).

[References]

[1] Wang X, Zhang L, Yuan H R, Li Y J, Zuo X Y, Li J W, et al. Resistance characteristics of non-Newtonian fluid flow in the process of pipe suction of pig manure. Chinese Journal of Environmental Engineering, 2021; 15(1): 368–374. (in Chinese)

[2] Dong B C, Song C J, Li H B, Lin A J, Wang J C, Li W. Life cycle assessment on the environmental impacts of different pig manure management techniques. Int J Agric & Biol Eng, 2022; 15(3): 78–84.

[3] Dong S S, Sui B, Shen Y J, Meng H B, Zhao L X, Ding J T, et al. Investigation and analysis of the linkage mechanism and whole process cost of livestock manure organic fertilizer. Int J Agric & Biol Eng, 2020; 13(2): 223–227.

[4] Tian L, Shen F, Yuan H R, Zou D X, Liu Y P, Zhu B N, et al. Reducing agitation energy-consumption by improving rheological properties of corn stover substrate in anaerobic digestion. Bioresource Technology, 2014; 168: 86–91.

[5] Mao L W, Zhang J X, Dai Y J, Tong Y. Effects of mixing time on methane production from anaerobic co-digestion of food waste and chicken manure: Experimental studies and CFD analysis. Bioresource Technology, 2019; 294: 122177. doi: 10.1016/j.biortech.2019.122177.

[6] Gao Y H, Zhang C A, Dong J J. Research progress on fertilizer application of biogas residue and liquid. Shandong Agricultural Sciences, 2011; 1(6): 71–75. (in Chinese)

[7] Ding J T, Shen Y J, Ma Y R, Meng H B, Cheng H S, Zhang X, et al. Study on dynamic sorption characteristics of modified biochars for ammonium in biogas slurry. Int J Agric & Biol Eng, 2020; 13(1): 234–240.

[8] Zheng J, Qi X Y, Yang S H, Shi C, Feng Z J. Effects and evaluation of biogas slurry/water integrated irrigation technology on the growth, yield and quality of tomatoes. Int J Agric & Biol Eng, 2022; 15(5): 123–131.

[9] Balsari P, Airoldi G, Gioelli F. Improved recycling of livestock slurries on maize by means of a modular tanker and spreader. Bioresource Technology, 2005; 96(2): 229–234.

[10] Gioelli F, Balsari P, Dinuccio E, Airoldi G. Band application of slurry in orchards using a prototype spreader with an automatic rate controller. Biosystems Engineering, 2014; 121: 130–138.

[11] Rodhe L, Etana A. Performance of slurry injectors compared with band spreading on three Swedish soils with Ley. Biosystems Engineering, 2005; 92(1): 107–118.

[12] Wang J W, Pan Z W, Yang X L, Liu Y U, Zhang C F, Wang J F. Design and experiment of rotary converter of liquid fertilizer. Transactions of the CSAM, 2014; 45(10): 110–115. (in Chinese)

[13] Zhou W Q, Sun X B, Liu Z M, Qi X, Jiang D X, Wang J W. Simulation analysis and test of interaction between pricking hole needle body of liquid fertilizer hole applicator and soil. Transactions of the CSAM, 2020; 51(4): 87–94. (in Chinese)

[14] Yang Z D, Wang T G, Lan Y, Zhao G H. Study of design and test on wheel-type liquid fertilizer deep machinery. Journal of Agricultural Mechanization Research, 2017; 39(4): 139–143. (in Chinese)

[15] Li W Z, Yuan H, Liu H X, Wang M, Li W T, Yin L L. Biogas slurry fertilizer application for dark irrigation. Transactions of the CSAM, 2014; 45(11): 75–80. (in Chinese)

[16] Liu H X, Xu G W, Jia R, Li Y L. Operating principle and structural optimization of impulse type anti-blocking distribution device for biogas manure. Transactions of the CSAE, 2015; 31(22): 32–39. (in Chinese)

[17] Zhai X D, Denka K I, Wu B X. Investigation of the effect of intermittent minimal mixing intensity on methane production during anaerobic digestion of dairy manure. Computers and Electronics in Agriculture, 2018; 155: 121–129.

[18] Schneider N, Gerber M. Rheological properties of digestate from agricultural biogas plants: An overview of measurement techniques and influencing factors. Renewable and Sustainable Energy Reviews, 2020; 121: 109709. doi: 10.1016/j.rser.2020.109709.

[19] Wu B X, Chen S L. CFD simulation of non-Newtonian fluid flow in anaerobic digesters. Biotechnology and Bioengineering, 2008; 99(3): 700–711.

[20] Standard methods for the examination of water and wastewater. Washington, DC, USA: American Public Health Association, 2005.

[21] Markis F, Baudez J, Parthasarathy R, Slatter P, Eshtiaghi N. The apparent viscosity and yield stress of mixtures of primary and secondary sludge: Impact of volume fraction of secondary sludge and total solids concentration. Chemical Engineering Journal, 2016; 288: 577–587.

[22] Luo T Q. Fluid Mechanics. 4th. Beijing, China: China Machine Press, 2020.

[23] Liu Y Q, Chen J J, Song J, Hai Z, Lu X H, Ji X Y, et al. Adjusting the rheological properties of corn-straw slurry to reduce the agitation power consumption in anaerobic digestion. Bioresource Technology, 2019; 272: 360–369.

[24] Hreiz R, Adouani N, Fünfschilling D, Marchal P, Pons M. Rheological characterization of raw and anaerobically digested cow slurry. Chemical Engineering Research and Design, 2017; 119: 47–57.

[25] Schneider N, Gerber M. Rheological properties of digestate from agricultural biogas plants: An overview of measurement techniques and influencing factors. Renewable and Sustainable Energy Reviews, 2020; 121: 109709. doi: 10.1016/j.rser.2020.109709.

[26] Slatter P T. The rheological characterisation of sludges. Water Science and Technology, 1997; 36(11): 9–18.

[27] Tang B, Zhang Z. Essence of disposing the excess sludge and optimizing the operation of wastewater treatment: Rheological behavior and microbial ecosystem. Chemosphere, 2014; 105: 1–13.

[28] Hong E, Herbert C M, Yeneneh A M, Sen T K. Rheological characteristics of mixed kaolin-sand slurry, impacts of pH, temperature, solid concentration and kaolin-sand mixing ratio. International Journal of Environmental Science and Technology, 2016; 13(11): 2629–2638.

[29] Wei L L, Ren Y M, Zhu F Y, Xia X H, Xue C H, Yang H Z, et al. Horizontal flow reactor optimization for biogas recovery during high solid organics fermentation: Rheological characteristic analyses. Journal of Water Process Engineering, 2021; 40: 101776. doi: 10.1016/j.jwpe.2020.101776.

[30] Servati P, Hajinezhad A. CFD simulation of anaerobic digester to investigate sludge rheology and biogas production. Biomass Conversion and Biorefinery, 2020; 10(4): 885–899.